Songklanakarin J. Sci. Technol.
35 (6), 727-738, Nov. - Dec. 2013

SJST SONGKLANAKARIN JOURNAL OF SCIENCE AND TECHNOLOGY
http://www.sjst.psu.ac.th

Original Article

Evaluation of carbaryl sorption in alluvial soil

Naba Kumar Mondal*, Soumya Chattoraj, Bikash Sadhukhan, and Biswajit Das

Department of Environmental Science, University of Burdwan, Golapbag, Burdwan, West Bengal, 713104 India

Received 22 October 2012; Accepted 20 August 2013

Abstract

This study investigated the adsorption potential of carbaryl onto alluvial soil. Parameters that influence the adsorption process such as pH, adsorbent dose, initial carbaryl concentration, stirring rate, particle size, contact time and temperature were studied in a batch process. The carbaryl adsorption capacity was at maximum at pH 6 for an initial concentration of 20 ppm. Adsorption equilibirium time was observed in 180 min. Equilibrium adsorption data was best fitted with Freundlich isotherm and pseudo-first order kinetic model, respectively. The adsorbent was characterized by X-ray diffraction spectrum, Fourier transform infrared spectroscopy and scanning electron microscopy. The experiment performed indicated that the adsorption capacity of carbaryl was significantly correlated with particle size, organic matter and pH of the soil. Therefore, the possibility for carbaryl to contaminate underground water may be greater in the presence of low organic matter content.

Keywords: adsorption, alluvial soil, carbaryl, adsorption isotherms, thermodynamic parameters, adsorption kinetics, ANN

1. Introduction

The use of insecticides is one of the major factors behind the increase in agricultural productivity in the 20th century (Van Emden, 1996). Carbaryl (1-naphthyl methyl carbamate) is a wide-spectrum chemical in the carbamate family used chiefly as an insecticide. Carbaryl disrupts the normal functioning of the insect nervous system and may cause toxicity by contact or ingestion (Tomlin, 2000). Carbaryl kills both targeted (e.g. malaria-carrying mosquitoes) and beneficial insects (e.g. honey bees), as well as crustaceans and earthworms (Gupta and Saxena, 2003). It is a cholinesterase inhibitor, toxic to fish, birds and mammal nervous systems, likely to be human carcinogenic (U.S. Environment Agency, 2003), mutagenic (Delescluse *et al*., 2001) and reproductive toxic (Xia *et al*., 2005). Its toxicity to non -target rats and mice was determined to be high. Application of carbaryl is done by foliar spray, through drip irrigation and also by soil drenching around individual vines. Thus, directly or indirectly, the soil system appears as the ultimate sink of carbaryl residues. Once it enters into soil system, it may get partitioned between soil solid and solution phases and maintains dynamic equilibrium. Therefore, the sorption behavior governs the fraction of residues present in soil solution phase, in which it is available for leaching and groundwater contamination. Thus the interaction of carbaryl with the soil thus becomes extremely important. The half-life of carbaryl ranges from four days in aerobic soils (Miller, 1993a) to 72.2 days in anaerobic soils (Miller, 1993b), which may culminate when either during flood or with increased dose. Direct or indirect application of carbaryl in variety of soil textures causing different patterns of adsorption process and affects other related processes such as transport, degradation, volatilization, bioaccumulation, that influence the final fate of carbaryl in the soil environment (Gao *et al.,* 1998) Hence the extent of surface water and ground water contaminations is there by affected. It is worth-mentioning that various organic and inorganic compounds in varying composition coupled with surface activity are components of soils. They can bind carbaryl and reduce the bioavailability (Torrents and Jayasundra, 2012). Carbaryl adsorption on the soil particles and retention solely depends on the clay

* Corresponding author.
Email address: nkmenvbu@gmail.com

fraction of soil and chemical properties of both soil and carbaryl (USDA, 1998). Previous study shows that the carbaryl sorption on bentonite clay is greater than that on kaolinite (Rajagopal *et al*., 1984) and the ability of smectite to adsorb organic contaminants and pesticides from aqueous solution is influenced by the exchangeable cations, as well as structural charge and its origin (Haderlein *et al.,* 1996; Boyd *et al.,* 2001). Aly *et al*. (1980) studied sorption of carbaryl and found that Ca^{2+}-bentonite exhibited the highest affinity for carbaryl, followed by an alluvial soil, calcareous soil, and calcite. Although carbaryl is subject to alkaline hydrolysis, its degradation by calcite was not noted. Sheng *et al*. (2001) evaluated the potential contribution of smectite and organic matter to pesticide retention in soils, and concluded that homoionic K^{+}-smectite was a more effective sorbent than muck soil for carbaryl. Chattoraj *et al.* (2013) predicted that carbaryl is moderately adsorbed in alluvial soil.

Artificial neural networks (ANN) are a possible alternative modeling tool for various processes and operations involving nonlinear multivariable relationships. Among several types of ANN architecture multilayer perceptron (MLP) is observed to be most common for chemical processes (Pandharipande *et al.*, 2013). Basically this is a feed forward neural network, has a multilayer structure consisting of one input and output layer and at least one hidden layer in-between. The number of nodes in input and output layers is decided by the number of independent and dependent parameters defining the process whereas the selection of number of hidden layers is dependent on the complexity of the process. The nodes in successive layers are connected with each other through connectionist constants called as weights. The data is transferred in the form of array of matrix from input layer to output layer through hidden layers. The output signal is compared with the target value to generate error signal. By adjusting the weights using appropriated algorithm, training of the network is to be carried out to minimize the error (Rumelhart and McClelland, 1986; Anderson, 1999; Pandharipande 2004).

Various researchers (e.g. Meenakhsipriya *et al*., 2009) used ANN models to predict adsorption efficiency. In the present work, the sorption behavior of carbaryl in alluvial soil was explored for determining the persistence in the environment. The effects of various experimental parameters such as pH, adsorbent dose, initial carbaryl concentration, stirring rate, particle size, contact time and temperature on adsorption of carbaryl were investigated. Adsorption isotherms and thermodynamic parameters were also evaluated which is finally tested by using ANN Model.

2. Materials and Methods

2.1 Chemicals

4-nitrobenzene diazonium fluoborate (Sigma Aldrich) A.R. (99.9% purity) was used as the main reagent and a fresh 0.03% (W/V) methanolic solution was made. An analytical standard pure sample of carbaryl was obtained by the recrystalization of a technical grade sample supplied by Bayer. Extraction solvent was Optima grade methanol. Stock solutions were made in A.R. grade $CaCl_2$, A.R. grade NaOH and subsequent dilutions were made in methanol. All standard solutions were kept at room temperature of the laboratory.

2.2 Soil

Soil (0-30 cm) used in this study was collected from the banks of river Bhagirathi in West Bengal, India owing to its high alluvial soil content and low permeability. The alluvial soil (inceptisol) sample was not purified prior to usage. The soil sample was air dried for few days and grinded into different particle size using different metal sieves having different mesh size and stored in clean glass jars prior to experiment. The pH values of the soil was measured in a 1/1 ratio (w/v) of soil/water. The physico–chemical characteristics of the soil are listed in Table 1.

2.3 Adsorbent characterization

Adsorbent characterization was performed by means of spectroscopic and quantitative analysis. The surface area of the adsorbent (alluvial soil) was determined by Quantachrome surface area analyzer (model NOVA 2200C). The pH of aqueous slurry was determined by soaking 1 g of alluvial soil in 50 ml distilled water, stirred for 24 hrs and filtered and the final pH was measured. The % of clay, silt, and sand was determined by hydrometric method (Saha *et al.,* 2010). The cation exchange capacity (CEC) of the alluvial soil sample was determined by the ammonium acetate method (Rhoades, 1982). The concentrations of sodium and potassium were

Table 1. Physico-chemical characteristics of soil.

Parameters	Value
Silt (%)	9.1
Sand (%)	81
Clay (%)	3.08
Organic carbon (%)	1.6
pH	6.2
CEC ($cmol^{+} kg^{-1}$)	14.2
Bulk density (gcm^{-3})	1.84
Moisture (%)	3.298
Specific gravity	1.21
Porosity (%)	40.21
Particle density ($g\ cm^{-3}$)	2.55
Al_2O_3 (%)	6.9
Na^{+} ($mg\ L^{-1}$)	62.1
K^{+} (mgL^{-1})	16.7
Ca^{2+} ($mg\ L^{-1}$)	0.4
Mg^{2+} ($mg\ L^{-1}$)	11.6
PO_4^{3-} ($mg\ L^{-1}$)	0.91

estimated by Flame Photometer (Model No. SYSTRONICS 126) while magnesium, calcium, and residual copper (II) concentration were determined by atomic absorption spectrophotometer (Model No.GBC HG 3000). For stirring purpose magnetic stirrer (TARSONS, Spinot digital model MC02, CAT No.6040, S. No.173) is used. The Fourier transform infrared (FTIR) spectra of alluvial soil before and after carbaryl adsorption were recorded with Fourier transform infrared spectrophotometer (PERKIN-ELMER, FTIR, Model-RX1 Spectrometer, USA) in the range of 400-4,400 cm^{-1}. X-ray diffraction analysis of the adsorbent was carried out using X-ray diffractometer equipment (Model Philips PW 1710) with a Cobalt target at 40 kV. In addition, scanning electron microscopy (SEM) analysis was carried out using a scanning electron microscope (HITACHI, S-530, Scanning Electron Microscope and ELKO Engineering, B.U. BURDWAN) at 25 kV to study the surface morphology of the adsorbent.

2.4 Determination of point zero charge

The point of zero charge of the adsorbent was determined by the solid addition method (Mondal, 2010). A 50 ml of 0.1 M KNO_3 solution transferred into a series of 100 ml conical flask. The initial pH (pH_0) values of the solution were adjusted from 1.0 to 10.0 by adding either 0.1(N) of HNO_3 or 0.1(N) KOH then 1.5 g of soil was added to each flask which was securely capped immediately. Then the flask were placed into constant temperature water bath shaker and shaken for 24 hrs. The pH values of the supernatant liquid were noted after 24 hrs. The result is presented in Figure 1.

2.5 Batch experiments

The batch tests were carried out in 250 mL volumetric flask with 20 mL of working volume stock solution of carbaryl. The stock solution was made in 0.02 (M) $CaCl_2$ solutions to obtain six different concentrations that were used to the experiment. 2 g air dried alluvial soil sample was added to the solution. The flasks were agitated at a speed of 250 rpm for 120 minutes in a magnetic stirrer (Digital MCO2) at 303±1 K. The influence of pH (range 2.0–12.0), adsorbent dose (ranges 0.5, 1, 1.5, 2 , 2.5, 3, 4 g/20 mL) initial carbaryl concentration (0.4, 1, 2, 5, 10, 20, 24 ppm), stirring rate (60, 150, 250, 400, 500, 600 rpm), particle size (50, 100, 150, 250 μm) contact time (ranges 30, 60, 90, 120, 180, 240, 300 min) and temperature (293, 303, 313, 323, 333 K) were evaluated during the present study. Samples were collected from the flasks at predetermined time intervals for analyzing the residual carbaryl concentration. The residual carbaryl concentration in each flask was determined using the single beam UV-VIS spectrophotometer. The spectrophotometric determination of carbaryl was done by following the method of Sainsbury and Miscus (1964) with some modifications. 5 ml (0.5N) NaOH was added to 5 ml aliquot taken in a 20 ml volumetric flask followed by 5 ml of 0.03% (W/V) methanolic solution of p-nitrobenzene diazonium fluoborate. The mixture was then diluted to 20 ml with methanol and after 20 min absorbance of the greenish–blue color solution was measured at 590 nm using a spectrophotometer (Bausch-Lomb Spectronic 20). The amount of carbaryl adsorbed per unit adsorbent (mg carbaryl per g adsorbent) was calculated according to a mass balance on the carbaryl concentration using the following Equation 1.

$$q_s = \frac{(C_i - C_f) \times V}{m} \quad (1)$$

Where C_i is the initial carbaryl concentration (mgL^{-1}), C_f is the equilibrium carbaryl concentration in solution (mgL^{-1}), V is the volume of the solution (L) and m is the mass of the soil in g. The (%) adsorption of carbaryl was calculated using the following equation

$$\%Adsorption = \frac{(C_i - C_f)}{C_i} \times 100 \quad (2)$$

The soil sorption coefficients K_c (mLg^{-1}) and Koc were then calculated as $K_c = C_a/C_f$ and $Koc = K_c \times 1000/OC$ where OC is the organic carbon content of the soil ($g\ kg^{-1}$) (data not given). Control experiments were performed without the addition of adsorbent confirmed that the sorption of carbaryl on the walls of flasks was negligible.

2.6 Statistical analysis

In order to ensure the accuracy, reliability, and reproducibility of the collected data, all adsorption experiments were performed in triplicate, and the mean values were used in data analysis. Relative standard deviations were found to be within ±3%. Microsoft Excel 2007 program was employed for data processing. Non-linear regression analysis using Origin Pro 8.0 software was employed to determine the isotherm parameters and kinetic constants.

Due to the inherent bias resulting from linearization, three different error functions of non-linear regression basin, sum of the square of the errors (SSE), sum of the absolute errors (SAE) and chi-square (χ^2), were employed in this study to find out the best-fit isotherm model to the experimental equilibrium data. SSE is given as:

$$SSE = \sum_{i=1}^{n} \left(q_m - q_{exp}\right)_i^2$$

Here, q_m and q_{exp} are the calculated and the experimental value of the equilibrium adsorbate solid concentration in the

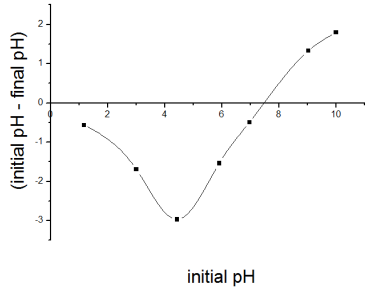

Figure 1. pH of zero charge of soil.

solid phase (mg/g), respectively, and n is the number of the data point. SAE is given as:

$$\text{SAE} = \sum_{i=1}^{n} \left| q_m - q_{\exp} \right|_i$$

Chi-square (χ^2) is given as:

$$\chi^2 = \sum_{i=1}^{n} \left[\frac{\left(q_{\exp} - q_m \right)_i^2}{q_m} \right]_i$$

The respective values are given in the Table 3. As shown in Table 3, the Freundlich adsorption isotherm model yielded best fit to the experimental equilibrium adsorption data than the Langmuir isotherm model for carbaryl adsorption according to the values of R^2, χ^2, SSE and SAE.

3. Results and Discussion

3.1 Soil characterization

The soil was found to be stable in water, dilute acids and bases. The adsorbent behaves as neutral at pH zero change. To understand the adsorption mechanism, it is necessary to determine the point of zero charge (pHzpc) of the adsorbent. Adsorption of cation is favored at pH>pHzpc, while the adsorption of anion is favoured at pH<pHzpc (Mondal, 2010). The point of zero Charge is 7.2 (Figure 1).

3.2 Adsorbent characterization

3.2.1 FTIR analysis

The FTIR spectral analysis is important to identify the characteristic functional groups on the surface of the adsorbent, which are responsible for adsorption of carbaryl molecule (Sheng, 2004; Ahalya, 2005). The FTIR spectrum of soil was recorded to obtain the information regarding the stretching and bending vibrations of the functional groups which are involved in the adsorption of the adsorbate molecule. The FTIR spectral analysis at before adsorption (Figure 2a) of the soil shows distinct peaks at 4,300, 3,449, 2,365, 2,345, 1,638, 1,408, 1,102, 1,030, 777, 694, 506, 533, 470 cm^{-1}. Among them the strong adsorption band at 3,449 cm^{-1} indicates the presence of amide group (-NH_2), the peak at

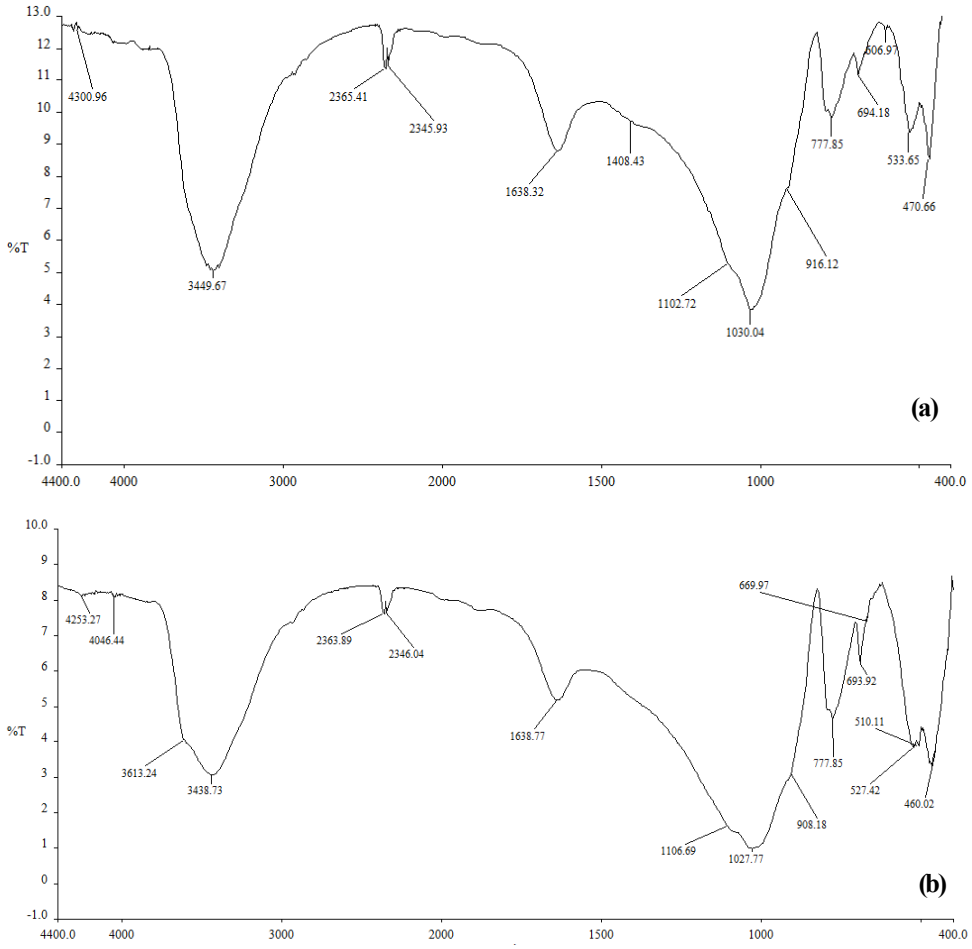

Figure 2. (a) FTIR spectra of soil before adsorption of carbaryl. (b) FTIR spectra of soil after adsorption of carbaryl.

1,408 is due to aromatic C=C stretching vibration, absorbance at 777 cm^{-1} and 694 cm^{-1} is due to aromatic C-H. After carbaryl adsorption The –NH group is shifted to lower frequency (3,438 cm^{-1}) and a strong band at 3,613 cm^{-1} is appeared, which indicates the presence of –OH group. Thus, it can reasonably be concluded that -OH and -NH_2 groups may be the main binding sites for carbaryl adsorption to soil.

3.2.2 SEM analysis

SEM analysis is another useful tool for the surface morphology of an adsorbent fundamental physical proportion of the adsorbent (Chadrudee *et al.*, 2011). The porous and irregular surface structure of the adsorbent can be clearly observed in the SEM images shown in Figure 3a. Further the pores on the surface of the adsorbent are highly heterogeneous as shown in Figure 3b. The heterogeneous pores and cavities provided a large exposed surface area for the adsorption of the carbaryl. The size of pores is indicative of the expected adsorption of the carbaryl molecule onto the surface of the soil.

3.3 X-ray diffraction analysis

X–ray data is shown in Figure 4. It is clearly revealed that the adsorbent is amorphous and porous in nature.

3.3.1 Effect of pH

pH has been recognized as one of the important factor in carbaryl adsorption (Murthy and Raghu, 1991). The structural stability of the carbaryl molecule is also associated with pH, at alkaline medium carbaryl breaks down into CO_2 and 1-Napthol. Adsorption process is directly related with competition ability of hydrogen ions to active sites on the adsorbent surface. The adsorption of carbaryl by soil was noted to increase with the increase of pH of the carbaryl solution appreciably up to pH6. A further increase in carbaryl sorption between pH 6.0 to 12.0 adsorption decreases (Figure 5a). So carbaryl binds more readily to acidic soil (Rajagopal *et al.*, 1984). Since the optimum pH for carbaryl adsorption was found to be 6, it was kept constant for further studies.

3.3.2 Effect of adsorbent dose

Adsorbent dose has an influencing power in sorption process since it determines the sorption capacity of an adsorbent for a given initial concentration of the adsorbate at the operation conditions. The adsorption profile of carbaryl versus different concentration of adsorbate (range of 0.5-4 g/20 ml) is shown In Figure 5b. It was observed that the percentage of carbaryl adsorption increased with increase of adsorbent dose. Such a trend is mostly attributed to an increase in the sportive surface area and the availability of more active adsorption sites (Nasuha *et al.*, 2010). Although the percentage adsorption of carbaryl increased with increase of adsorbent dose, the maximum carbaryl adsorption was observed at 3 g and further increase in adsorbent dose did not significantly change the adsorption yield. This is due to the binding of almost all the carbaryl molecule to adsorbent surface and the establishment of the equilibrium between the carbaryl molecule on the adsorbent and in the solution (Akar *et al.*, 2009). Hence in the present study 3 g adsorbent/20ml carbaryl solution was employed for further experiments.

3.3.3 Effect of initial concentration

The rate of adsorption is a function of the initial concentration of the adsorbate, which makes it an important

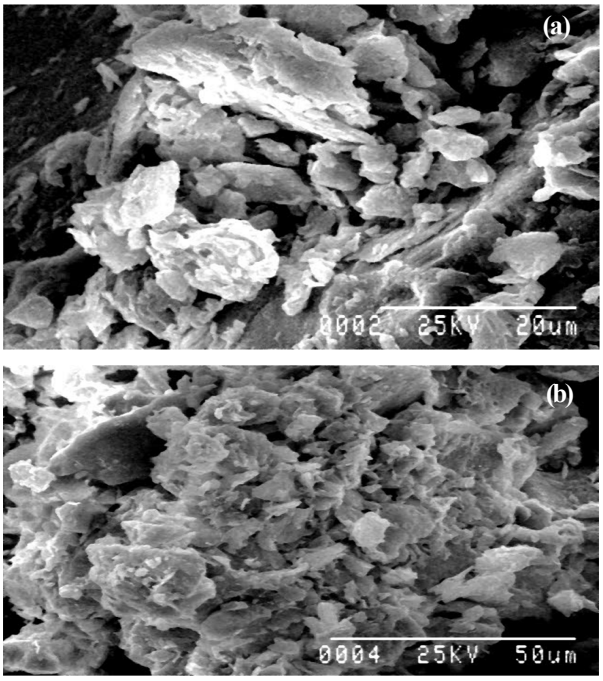

Figure 3. (a) SEM of after adsorption of carbaryl onto soil. (b) SEM of after adsorption of carbaryl onto soil.

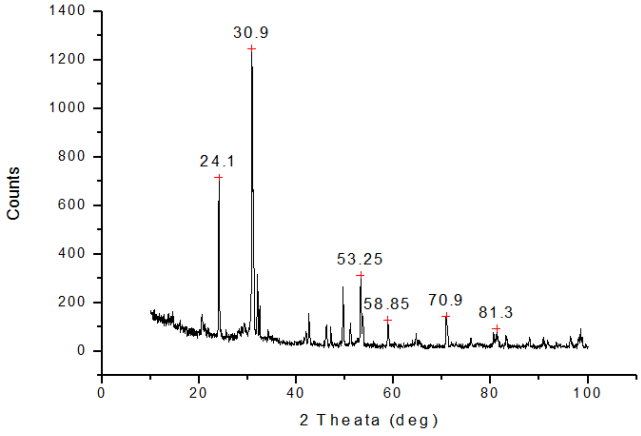

Figure 4. X-ray diffraction spectrum of alluvial soil.

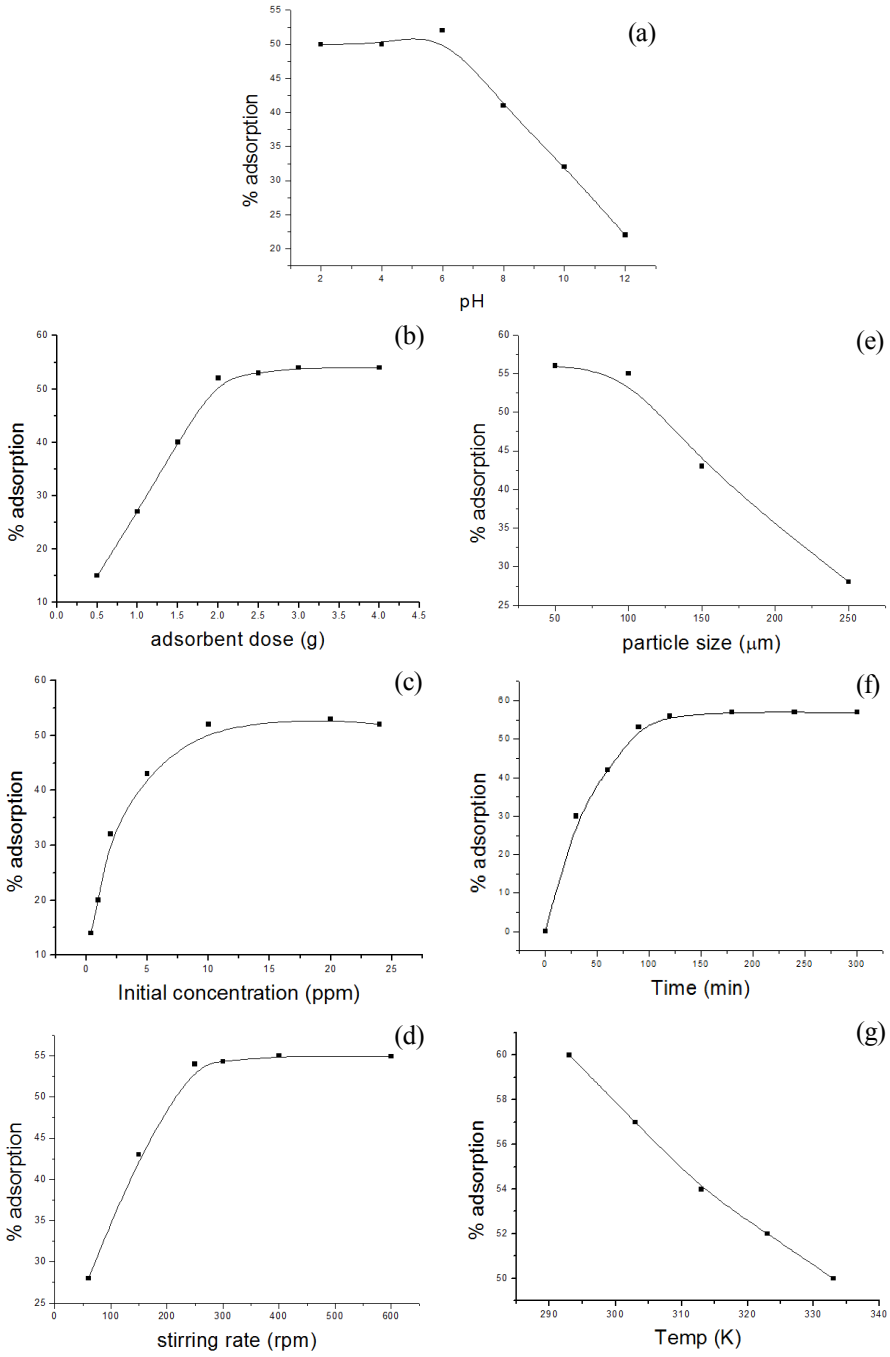

Figure 5. (a) Effect of pH on adsorption of carbaryl by soil. Experimental conditions: adsorbent dose 2 g, initial carbaryl concentration 10 ppm, stirring rate 250 rpm, pH 6, temperature 303 K, particle size 100 μm, contact time 120 min.
(b) Effect of adsorbent dose on adsorption of carbaryl by soil. Experimental conditions: adsorbent dose 2 g, stirring rate 250 rpm, initial carbaryl concentration 10 ppm, pH 6, temperature 303 K, particle size 100 μm, contact time 120 min.
(c) Effect of initial carbaryl concentration on adsorption by soil. Experimental conditions: adsorbent dose 3g, stirring rate 250 rpm, pH 6, temperature 303 K, particle size 100 μm, contact time 120 min.
(d) Effect of stirring rate on adsorption of carbaryl by soil. Experimental conditions: adsorbent dose 3 g, pH 6, temperature 303 K, initial carbaryl concentration 20 ppm, particle size 100 μm, contact time 120 min.
(e) Effect of particle size on adsorption of carbaryl by soil. Experimental conditions: adsorbent dose 3 g, stirring rate 400 rpm, pH 6, temperature 303 K, initial carbaryl concentration 20 ppm, contact time 120 min.
(f) Effect of contact time on adsorption of carbaryl by soil. Experimental conditions: adsorbent dose 3 g, stirring rate 400 rpm, pH 6, temperature 303 K, initial carbaryl concentration 20 ppm, particle size 50 μm.
(g) Effect of temperature on adsorption of carbaryl by soil. Experimental conditions: adsorbent dose 3 g, stirring rate 400 rpm, pH 6, initial carbaryl concentration 20 ppm, contact time 180 min, particle size 50 μm.

factor to be considered for effective adsorption. The effect of different initial carbaryl concentration on the adsorption of carbaryl onto soil is shown on Figure 7. It is evident from the Figure 5c that the percentage adsorption of carbaryl increased with increase in initial concentration of carbaryl (Chattoraj *et al.,* 2013). After certain concentration (20 ppm) there is no significant change in the adsorption yield. This can be explained that all adsorbents have a limited number of active sites, which become saturated at a certain concentration (Akar *et al*., 2009).

3.3.4 Effect of stirring rate

Studies on the effect of stirring rate were conducted by varying speed from (60-600 rpm) at pH 6 with adsorbent dose 3 g/20 ml and contact time 120 min. The influence of stirring rate on the extent of adsorption is shown in Figure 5d. It is revealed from the above figure that the carbaryl adsorption is a function of stirring rate. Carbaryl adsorption increases with the increase of stirring rate (Jana and Das, 1997). The percentage adsorption is less at lower stirring rate and increases with stirring rate up to 400 rpm and there after it remains more or less constant (Figure 5d) The s-shaped curve indicates multilayer adsorption and the carbaryl molecule binds the soil surface with availability of new sites to the solvent as adsorption takes place (Giles *et al*., 1960). The reason for the increase in efficiency is that at higher speeds better contact between the adsorbent and adsorbate is possible (Tembhurkar and Dongre, 2006). The adsorption extent for stirring rate after 400 rpm does not show any significant increase and hence stirring rate 400 rpm was considered for further studies.

3.3.5 Effect of particle size

Studies on the effect of particle size were conducted by varying particle size (50-250 μm) at a speed of 400 rpm, pH 6 with adsorbent dose 3 g/20 ml, contact time 120 min and 20 ppm initial concentration of carbaryl. The influence of particle size on the extent of adsorption is shown in Figure 5e. Data obtained from the experiments are clearly indicated that carbaryl adsorption decreased with increase particle size. The observed decrease in the adsorption capacity with increase of particle size from (50-250 μm) indicates that low particle size favors the carbaryl adsorption process on to soil. These results indicate that as contact area increases adsorption of carbaryl process also increases with a maximum at 50 μm.

3.3.6 Effect of contact time

It is essential to evaluate the effect of contact time required to reach equilibrium for designing batch adsorption experiments. Therefore the effect of contact time on adsorption of carbaryl was also investigated. The uptake of carbaryl as a function of contact time is shown in Figure 5f. It shows that adsorption of carbaryl increased with rise in contact time up to 180 min. Further increase in contact time did not enhance the carbaryl adsorption process. Slow increase of adsorption at initial stage indicates that interaction between carbaryl and soil was not by an ion exchange (Bunzl *et al*., 1976) and the equilibrium is reached within 240 minutes. Similar observation is shown by Jana and Das (1997).

3.3.7 Effect of temperature

Temperature is also an additional factor which has an influencing power in any adsorption process. So batch adsorption experiments were carried out at different temperature ranging from 293K to 333 K. Data obtained from the experiments are clearly indicate that carbaryl adsorption decreased with increase in temperature. The observed decrease in the adsorption capacity with increase of temperature indicates (Figure 5g) that indicates that low temperature favors the carbaryl adsorption process onto soil (Aly *et al*., 1980).

3.4 Adsorption isotherm

The Langmuir and Freundlich models were used to describe the equilibrium adsorption data at different temperatures. The linearized form of isotherms (Babu and Gupta, 2008) and their constants are given in Table 2. The experimental data obtained at equilibrium was fitted satisfactorily with Freundlich isotherm and is shown in Figure 6. The Freundlich isotherm reveals the multilayer adsorption. Similar observations have been shown by Joseph *et al*. (1974) and Jana and Das. (1997).

3.5 Adsorption kinetics

Two kinds of models were used to study the reaction pathways and potential rate limiting steps of the adsorption of carbaryl on to soil. The linearized form of adsorption kinetics (Guo *et al*., 2002) and their constants are presented in Table 3. From the table, it is confirmed that the adsorption of carbaryl onto alluvial soil followed the pseudo-First order reaction and is shown in Figure 7.

3.6 Activation energy and thermodynamics parameter

From the pseudo second order rate constant k_2 was determined (Table 3). The activation energy E_a for the adsorption of carbaryl onto soil was determined using the Arrhenius equation. By plotting $\ln k_2$ versus $1/T$, E_a was obtained from the slope of the linear plot (figure not shown). The value of E_a for adsorption carbaryl onto soil was 8.56 $kJmol^{-1}$. The magnitude of activation energy may give an idea about the type of sorption. There are two main types of adsorption: physical and chemical. The activation energy for physical adsorption is usually less than 40 kJ mol^{-1}, since the forces involved in physical adsorption are weak. Higher

Table 2. Adsorption isotherm constants for adsorption of carbaryl by soil at different temperatures.

Isotherm model	Equation	Parameter	Temperature					χ^2	SSE	SAE
			293K	303K	313K	323K	333K			
Langmuir isotherm	$\frac{C_f}{q_s}=\frac{C_f}{q_m}+\frac{1}{k_L q_m}$	q_m (μgg^{-1})	91	88	82	67	56			
		K_L(Lmg^{-1})	0.114	0.092	0.071	0.043	0.022	0.208	1.045	1.628
		R^2	0.9710	0.9434	0.9558	0.9653	0.9741			
Freundlich isotherm parameters	$\log q_s=\log k_f+(\frac{1}{n})\log c_f$	K_F(mgg^{-1})(Lmg^{-1})	2.75	2.63	2.23	2.11	1.76			
		1/n	1.427	1.411	1.023	1.007	1.004	0.1414	0.512	1.228
		R^2	0.9940	0.9982	0.9991	0.9984	0.9975			

q_s (mgg^{-1}) and c_f (mgL^{-1}) are the solid phase concentration and the liquid phase concentration of adsorbate at equilibrium respectively, q_m (mgg^{-1}) is the maximum adsorption capacity and k_L (Lmg^{-1}) and K_F (mgg^{-1}) (Lmg^{-1}) and is the adsorption equilibrium constant. n is the heterogeneity factor.

Table 3. Kinetic parameters for adsorption of carbaryl by soil.

Kinetic model	Equation	Parameter	Temperature				
			293K	303K	313K	323K	333K
Pseudo-first order kinetic model	$\ln(q_e-q_t)=\ln q_e-K_1 t$	q_{exp} (μgg^{-1})	80	78	65	55	47
		q_{cal} (μgg^{-1})	81.2	77.6	64.5	54.5	46.7
		K_1(min^{-1})	0.02763	0.2553	0.02303	0.02072	0.01876
		R^2	0.9980	0.9991	0.9998	0.9979	0.9991
Pseudo-second order kinetic model	$\frac{t}{q_t}=\frac{1}{k_2 q_e^2}+\frac{t}{q_e}$	q_{cal} (μgg^{-1})	76.3	69.7	60.1	46.5	36.9
		K_2($gmg^{-1}min^{-1}$)	0.04926	0.04212	0.03125	0.02514	0.02112
		R^2	0.941	0.936	0.928	0.933	0.956

q_t and q_s are the amount of Carbaryl adsorbed (mgg^{-1}) at time t and at equilibrium and K_1 (min^{-1}) is the Lagergren rate constant of first order adsorption and k_2 (gmg^{-1} min^{-1}) is the second order adsorption rate constant.

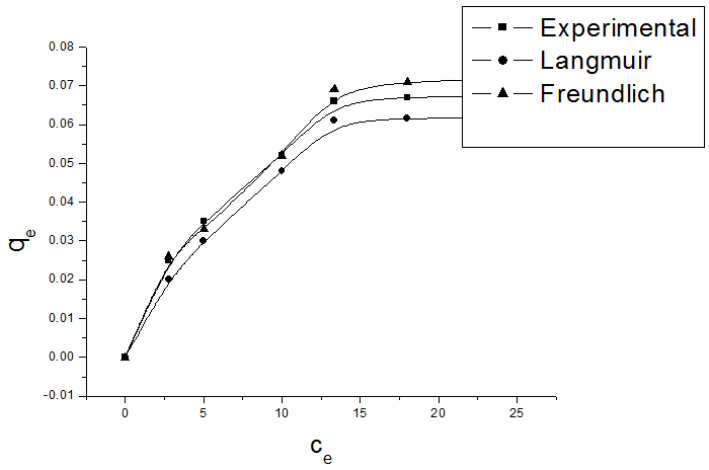

Figure 6. Comparison of the experimental data with the Langmuir and Freundlich isotherms for the adsorption of carbaryl on to soil.

values represent chemical reaction process as chemical adsorption is specific and involves forces much stronger than in physical adsorption. According to literature, the adsorption process of carbaryl onto soil may be phyisorption (E<8 $kJmol^{-1}$) (Bansal, 2004; Anirudhan and Radhakrishnan, 2008). The standard Gibb free energy (ΔG^0) for the adsorption of carbaryl onto soil at all temperatures was calculated obtained using the Equation 3.

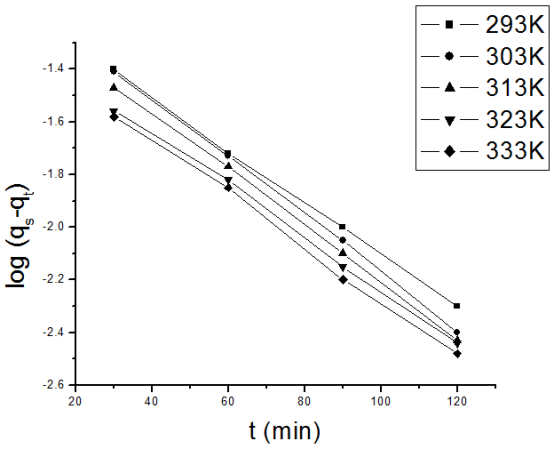

Figure 7. Pseudo-first-order-kinetic plots of carbaryl adsorption by soil at different temperatures. Experimental conditions: adsorbent dose 2 g, stirring rate 400 rpm, pH 6, particle size 50 ìm, initial carbaryl concentration 20 ppm.

$$\Delta G^0 = -RT \ln k_c \quad (3)$$

$$k_c = \frac{c_a}{c_f} \quad (4)$$

$$\Delta G^0 = \Delta H^0 - T\Delta S^0 \quad (5)$$

The values of enthalpy (ΔH^0) and entropy (ΔS^0) were determined from the slope and intercept of the plot of ΔG^0 vs. T (figure not shown) and are listed in Table 4. A negative value of free energy change shows that adsorption phenomenon is spontaneous in nature. Increase in value of ΔG^0 with increase in temperature indicates that lower temp makes the adsorption easier. The negative value of ΔH^0 suggests that adsorption process is exothermic. The negative value of ΔS^0 indicates that adsorption complex of carbaryl with soil were stable (Bansal, 2004).

3.7 Soil organic carbon partition coefficient and groundwater ubiquity score

Other parameters for the adsorption process soil organic carbon partition coefficient (K_{OC}), and groundwater ubiquity score (GUS) have been calculated by using Equations 6 and 7, respectively (Banerjee *et al*, 2008) as follows

$$K_{oc} = K_c \times \frac{100}{\%\ oc} \quad (6)$$

$$GUS = \log t_{1/2}\left[4 - \log(k_{oc})\right] \quad (7)$$

The GUS score is used to study the leaching behavior of pesticides which can be classified as leacher (GUS>2.8), transition (2.8>GUS>1.8) and non-leacher (GUS<1.8) (Papa *et al*., 2004). Under aerobic condition half life of carbaryl is found to be seven days. The calculated K_{OC} and $t_{1/2}$ values were put in the Equation 12 and the GUS was found to be 1.94. Hence, carbaryl is considered to be a chemical belonging to medium leaching potential category.

3.8 Artificial neural network approach

A Neural Network Toolbox Neuro Solution 5® mathematical software was used to determine carbaryl adsorption efficiency. Figure 8a shows the ANN Model used in the study. In this investigation 31 set of experimental data is used to estimate the percentage adsorption of carbaryl onto soil with using pH of the solution, initial carbaryl concentration, adsorption dose, contact time, stirring rate, and temperature. There is just one neutron in output layer which is the amount of adsorption predicted by ANN versus amount of adsorption obtained from experiments, during the training process. The plot of amount of adsorption predicted by ANN versus amount of adsorption obtained from experiments is shown in Figure 8b. The slope line 1.006 and amount R^2=0.953 show good training of the network.

4. Conclusions

In the present study carbaryl adsorption onto alluvial soil was investigated in a batch process. The adsorption studies were carried out as a function of pH, adsorbent dose, initial carbaryl concentration, stirring rate, particle size, contact time and temperature. The carbaryl adsorption capacity of the soil was found to be moderate and strongly dependent on its pH, particle size and organic matter contents. Therefore, application of carbaryl to strongly acidic soils with high organic matter contents may reduce its efficacy in controlling target organisms, at the same time, reducing the potential of ground water pollution through leaching. Further research on the fate of carbaryl in different soils would be very valuable in predicting ground water pollution resulting from carbaryl application.

Acknowledgements

The authors are grateful to faculty members and staff of the Department of Environment Science, University of Burdwan, India, for their help to initiate the work.

Table 4. Activation energy and thermodynamic parameters for adsorption of carbaryl by soil.

ΔG^0 (kj mol^{-1})					ΔH^0 (kj mol^{-1})	ΔS^0 (j mol^{-1}k^{-1})
293K	303K	313K	323K	333K	-19.89	-48
-5.31	-4.832	-4.028	-3.654	-3.479		

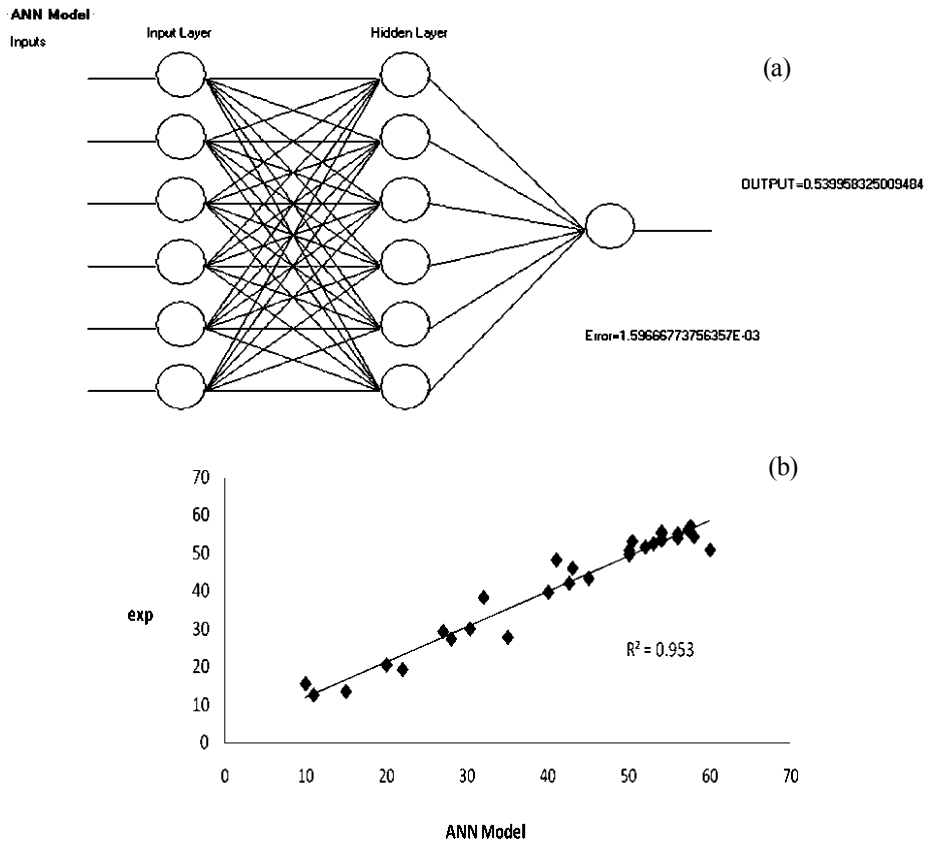

Figure 8. (a) Artificial neuron network model. (b) Experimental equilibrium data versus Ann model tested data.

References

Adhikari, M., Mondal, AK. and Ray, A. 1991. Sorption of Sumithion by Soil. Indian Society of Soil Science. 39, 680-684.

Ahalya, A., Kanamadi, R.D. and Ramachandra, T.V. 2005. Biosorption of Chromium (VI) from aqueous solutions by the husk of Bengal gram (Cicer arientinum). Electronic Journal of Biotechnology. 8(3), 258–264.

Akar, S.T., Özcan, A.S., Akar, T., Özcan, A. and Kaynak, Z. 2009. Biosorption of a reactive textile dye from aqueous solution utilizing an agro-waste. Desalination. 249, 757-761.

Aly, M.I., Barry, N., Kishk, F. and El-Sebae, A.H. 1980. Carbaryl adsorption on calcium-bentonite and soils. Soil Science Society of America Journal. 44, 1213-1215.

Anderson, J.A. 1999. An Introduction to Neural Networks, Prentice-Hall of India Pvt Ltd, New Delhi, India.

Anirudhan, T.S. and Radhakrishnan, P.G. 2008. Thermodynamics and kinetics of adsorption of Cu (II) from aqueous solution a new cation exchanger derived from tamarind fruit shell. The Journal of Chemical Thermodynamics. 40, 702- 709.

Babu, BV. and Gupta, S. 2008. Adsorption of Cr(VI) using activated neem leaves kinetic studies. Adsorption. 14 (1), 85–92.

Bailey, G.W. and White, J.L. 1970. Factors influencing the adsorption, desorption and movement of pesticides in Soil. Residue Review. 32, 39-92.

Banerjee, K., Patil, S.H., Dasgupta, S., Oulkar, D.P. and Adsule, P.G. 2008. Sorption of thiamethoxam in three Indian soils. Journal of Environmental Science and Health Part, B. 43(2), 151-156.

Bansal, O.P. 2004. Kinetics of interaction of three carbamate pesticides with Indian soils. Journal of Pest Management Science. 60, 1149–1155.

Boyd, S.A., Sheng, G., Teppen, B.J. and Johnston, C.T. 2001. Mechanisms for the adsorption of substituted nitrobenzenes by smectite clays. Environmental Science & Technology. 35, 4227-4234.

Bunzl, K., Schmidt, W. and Sansoni, B. 1976. Kinetics of ion exchange in soil organic matter IV. Adsorption and desorption of Pb^{2+}, Cu^{2+}, Cd^{2+}, Zn^{2+} and Ca^{2+} by peat. Journal of Soil Science. 27, 32-41.

Caro J.H., Freeman, H.P., Turner, B.C. 1974. Persistence to soil and losses in run off soil incorporated carbaryl in a small watershed. Journal of Agricultural and Food Chemistry 22, 860- 863.

Chadrudee, S., Chakkrit, U. and Pairat, K. 2011. Removal of

copper from aqueous solutions by adsorption using modify Zalacca edulis peel modify. Songklanakarin Journal of Science and Technology. 33 (6), 725-732.

Chattoraj, S., Sadhukhan, B. and Mondal, N.K. 2013. Predictability by Box-Behnken Model for carbaryl adsorption by soils of Indian Origin. Journal of Environmental Science and Health Part B. 48(8), 626-636.

Dang, S.V., Kawasaki, J., Abella, L.C., Auresenia, J.H., Habaki, H., Gaspillo, P.D., Hitoshi, K. and Hoa, T.D. 2009. Removal of arsenic from simulated groundwater by adsorption using iron-modified rice husk carbon. Journal of Water and Environment Technology. 7(2), 43–56.

Delescluse, C., Ledirac, N., Li, R., Piechocki, MP. Hines, RN., Gidrol, X. and Rahmani, R. 2001. Introduction of cytochrome P450 1A1 gene expression, oxidative stress, and genotoxicity by carbaryl and thiabendazole in transfected human HepG2 and lymphoblastoid cells. Biochemical Pharmacology. 61, 399-407.

Gao, J.P., Maguhn, J., Spitzauer, P. and Kettrup, A. 1998. Sorption of pesticides in the sediment of the Teufelesweiher pond (southern Germany). I: equilibrium assessments, effect of organic carbon content and pH. Water Research. 32(5), 1662-1672.

Giles, C.H., Macewan, T.H., Nakhwa, S.N. and Smith, D. 1960. Studies in adsorption, part XL. A system of classification of solution adsorption isotherms, and its use in diagnosis of adsorption and in measurement of specific surface areas of solids. Journal Chemical Society III, 3973-3993.

Gundogdu, A., Ozdes, D., Duran, C., Bulut, V.N., Soylak, M. and Senturk, H.B. 2009. Biosorption of Pb (II) ions from aqueous solution by pine bark (Pinus brutia Ten.). Chemical Engineering Journal. 153, 62–69.

Guo, Y., Qi, J., Yang, S., Yu, K., Wang, Z. and Xu, H. 2002. Adsorption of Cr (VI) on micro- and mesoporous rice husk-based active carbon. Materials Chemistry and Physics. 78, 132–137.

Gupta, S.K. and Saxena, P.N. 2003. Carbaryl-induced behavioural and reproductive abnormalities in the earthworm Metaphire posthuma: a sensitive model. Alternatives to laboratory Animals. 31(6), 587-593.

Haderlein, S.B., Weissmahr, K.W. and Schwarzenbach, R.P. 1996. Specific adsorption of nitroaromatic explosives and pesticides to clay minerals. Environmental Science and Technology. 30, 612-622.

HF, V.E. and Pealall, D.B. 1996. Beyond Silent spring, Chapman & Hall, London, UK. p 322.

Huang, P.M., Grover, R. and McKercher, R.B. 1984. Components and particle-size fractions involved in atrazine adsorption by soils. Soil Science. 28. 20-24.

Jana, T.K. and Das, B. 1997. Sorption of carbaryl (1-Napthyl N-Methyl Carbamate) by Soil. Bulletin of Environment Contamination and Toxicology. 59, 65-71.

Miller, N.E. 1993a. Metabolism of 14C-carbaryl under aerobic soil conditions, submitted in package of Rhone-Poulenc Ag Company, Department of Pesticide Regulation, Sacramento, Califonia, U.S.A., 169-268.

Miller, N.E. 1993b. Metabolism of 14C-carbaryl under anaerobic aquatic soil conditions, Department of Pesticide Regulation, Sacramento, Califonia, U.S.A., 169-268

Mondal, M. 2010. Removal of Pb (II) from aqueous solution by adsorption using activated tea waste. Korean Journal of Chemical Engineering. 27, 144-151.

Murthy, N.B.K. and Raghu, K. 1991, Fate of ^{14}C-carbaryl in soils as a function of pH. Bulletin of Environment Contamination and Toxicology. 46, 374-379.

Nasuha, N., Hameed, B., Azam, H.T. and Mohd, Din. 2010, Rejected tea as a potential low cost adsorbent for the removal of methylene blue. Journal of Hazardous Materials. 175, 126-132.

Pandharipande, S.L. 2004. Artificial Neural Network (FFEBPN), Elite-ANN software CD with case studies, Central Techno Publishers (Denett), Nagpur, India.

Rajagopal, B.S., Brahmaprakash, G.P., Reddy, B. R., Singh, U.D. and Sethunathan, N. 1984. Effect and persistence of selected carbamate pesticides in soils. Residue Reviews. 93, 87-203.

Rajagopal, B.S., Chendrayan, K., Reddy, R.B. and Sethunathen, N. 1983. Persistence of carbaryl in flooded soil and its degradation by soil enrichment cultures. Journal of Plant and Soil. 73, 35-45.

Rhoades, J.D. 1982. Cation exchange capacity, in: Methods of Soil Analysis Part 2. Chemical and Microbiological Properties, second ed., American Society of Agromony/ Soil Science Society of America, Madison, Wisconsin, U.S.A.

Rumelhart, D.E. and McClelland, C 1986. Back Propagation Training Algorithm Processing, M.I.T Press, Cambridge Massachusetts, U.S.A.

Saha, P. and Sanyal, SK. 2010. Assessment of the removal of cadmium present in wastewater using soil-admixture membrane. Desalination. 259, 131-139.

Sheng, G., Johnston, C.T., Teppen, B.J. and Boyd, S.A. 2001. Potential contributions of smectite clays and organic matter to pesticide retention in soils. Journal of Agricultural and Food Chemistry. 49, 2899-2907.

Sheng, P.X. ,Ting, Y.P., Chen, J.P. and Hong, L. 2004. Sorption of lead, copper, cadmium, zinc and nickel by marine algal biomass characterization of biosorptive capacity and investigation of mechanisms. Journal of Colloid and Interface Science. 275, 131–141.

Tembhurkar, A.R. and Dongre, S. 2006. Studies on fluoride removal using adsorption process. Journal of Environment Science & Engineering. 48, 151-156.

Tomlin. 2000. A World Compendium. The Pesticide Manual, 12th ed; C.D.S., Ed. British Crop Protection Council, Farnham, UK, pp. 67-68.

Torrents, A. and Jayasundra, S. 2012. The sorption of non-ionic pesticides on to clays and the influence of natural organic carbon. Chemosphere. 35(7), 1549-1565.

U.S. Environmental Protection Agency, Office of Pesticide Programs, Environmental Fate and Effect Division, 2003. Revised EFED Risk Assessment of Carbaryl in Support of the Registration Eligibility Decision, Washington DC., USA.

USDA NRCS. 1998. Soil quality concerns, pesticides, National Soil Survey Center in cooperation with the Soil Quality Institute, NRCS, USDA and the National Soil Tilth Laboratory, Agricultural Research Service (USDA).

Xia, Y., Cheng, S., Bian, Q., Xu, L., Collins, M.D., Chang, H.C., Song, L., Jiayin, Liu., Wang, J.S., Wang, X. 2005. Genotoxic effects of spermatozoa of carbaryl-exposed workers. Toxicological Sciences. 85, 615-623.

Nomenclature

A	Arrhenius constant
C_a	equilibrium Carbaryl concentration on the soil (mgL^{-1})
C_f	equilibrium Carbaryl concentration in solution (mgL^{-1})
C_i	initial Carbaryl concentration(mgL^{-1})
E_a	activation energy ($kj\ mol^{-1}$)
ΔG^0	Gibb's free energy ($kj\ mol^{-1}$)
ΔH^0	enthalpy of reaction ($kj\ mol^{-1}$)
H	initial adsorption rate ($mg\ g^{-1}\ min^{-1}$)
K_d	distribution coefficient for adsorption
K_f	Freundlich constant ($mgg^{-1)}(Lmg^{-1}$)
K_L	Langmuir constant (Lmg^{-1})
K_1	pseudo first order rate constant
K_2	pseudo second order rate constant
m	weight of the adsorbent (g)
n	Freundlich adsorption isotherm constant
q_s	equilibrium Carbaryl concentration on the soil (mgg^{-1})
q_m	maximum adsorption capacity (mgg^{-1})
R	universal gas constant ($8.314\ jmol^{-1}\ K^{-1}$)
R^2	correlation coefficient
ΔS^0	entropy of reaction ($j\ mol^{-1}k^{-1}$)
T	temperature (K)
V	volume (L)